Optimized double sweep Schwarz method by complete radiation boundary conditions

Seungil Kim[a,*], Hui Zhang[b]

[a]*Department of Mathematics and Research Institute for Basic Sciences, Kyung Hee University, Seoul 02447, Republic of Korea*
[b]*Key Laboratory of Oceanographic Big Data Mining & Application of Zhejiang Province, Zhejiang Ocean University, Zhoushan, Zhejiang 316022, China*

Abstract

We present an optimized double sweep nonoverlapping Schwarz method for solving the Helmholtz equation in semi-infinite waveguides. The domain is decomposed into nonoverlapped layered subdomains along the axis of the waveguide and local wave propagation problems equipped with complete radiation conditions for high-order absorbing boundary conditions are solved forward and backward sequentially. For communication between subdomains, Neumann data of local solutions in one domain are transferred to the neighboring subdomain in the forward direction and Dirichlet data are exploited in the backward direction. The complete radiation boundary conditions enable us to not only minimize reflection coefficients for most important modes in an optimal way but also find Neumann data without introducing errors that would be produced if finite difference formulas were used for computing Neumann data. The convergence of the double sweep Schwarz method is proved and numerical experiments using it as a preconditioner are presented to confirm the convergence theory.

Keywords: Helmholtz equation, nonoverlapping Schwarz method, complete radiation boundary condition, waveguide
2000 MSC: 65N30, 78M10

---

1. Introduction

In this paper, we study a nonoverlapping domain decomposition method for the Helmholtz equation in semi-infinite waveguides by using complete radiation boundary conditions (CRBCs) for an approximation to the exact radiation condition. We consider the time-harmonic wave propagation problem

$$\begin{aligned} &\Delta u + k^2 u = f \text{ in } \Omega, \\ &\frac{\partial u}{\partial \nu} = 0 \text{ on } \Gamma = \partial\Omega \setminus \bar{\Gamma}_0 \quad \text{and} \quad \frac{\partial u}{\partial \nu} = T(u) \text{ on } \Gamma_0. \end{aligned} \tag{1.1}$$

*Corresponding author
Email addresses: sikim@khu.ac.kr (Seungil Kim), huiz@zjou.edu.cn (Hui Zhang)

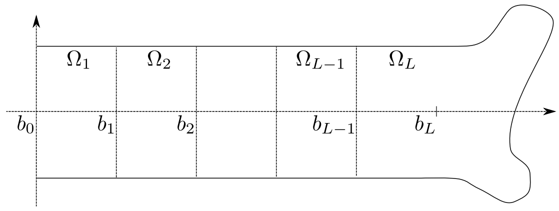

Figure 1: Decomposition of the locally perturbed waveguide with $b_0 = 0$ and $b_L = b$.

Here k is a positive wavenumber and Ω is a bounded domain in $\mathbb{R}^d$ with $d = 2$ or 3 obtained by truncating a semi-infinite waveguide Ω_∞ at $x = 0$ (the boundary at $x = 0$ is denoted by Γ_0), e.g., a cavity as seen in Figure 1. We assume that $\Omega_\infty \cap ((-\infty, b) \times \Theta) = (-\infty, b) \times \Theta$ for $b > 0$ and Θ is a smooth bounded domain in $\mathbb{R}^{d-1}$. Also, ν represents the outward unit normal vector on the boundary of Ω and T is the Dirichlet-to-Neumann (DtN) map employed for the radiation condition. $f \in L^2(\Omega)$ is a wave source with compact support in Ω. We remark that our analysis can be extended to more general domains such as junctions of semi-infinite waveguides.

The Helmholtz equation plays an important role in science and engineering since its solutions can describe behaviors of diverse time-harmonic wave fields arising from acoustics, electromagnetics and elastics. However, it is well-known that computing accurate numerical solutions to the Helmholtz equation, in particular in the high frequency regime, is challenging due to the highly oscillatory nature of solutions. Among others, the optimal or optimized Schwarz method (OSM) [1, 2, 3, 4, 5, 6] has been used successfully to treat the difficulty in computing numerical solutions to the Helmholtz equation of high wavenumber. While it can be used as a solver, OSM can also be a preconditioner for iterative Krylov space methods to speed up their convergence. In particular, the sweeping process for Helmholtz solvers initiated by [7] and independently invented and improved in [8] (which does not look like OSM) becomes attractive in OSM for the Helmholtz equation due to the advance of efficient absorbing boundary conditions such as PML. Analysis for these techniques can be found in the literature [9, 10, 11].

The optimized double sweep Schwarz method proposed in this work is motivated by the source transfer domain decomposition method (STDDM) proposed by [9] based on the PML method, in which computational domains are split in one way and the algorithm proceeds by solving subdomain problems in the forward direction to transfer wave sources generated in the former subdomains and in the backward direction to construct full wave expansions. We note that their idea to transfer wave sources generated in one domain to the next neighboring domain requires generously overlapped domains of local (subdomain) problems, which results in somewhat large number of unknowns for subdomain problems. The new method proposed in this paper reformulates the transparent boundary condition based on the DtN map such as (3.4) so that imposing this condition only requires to transfer a Neumann data of radiating wave fields from one subdomain to a neighboring subdomain. It is the important advantage that Neumann data of propagating waves can be computed in one subdomain and transferred to a neighboring but non-overlapped subdomain as opposed to STDDM requiring overlapped subdomains for local problems. This result leads to significant reduction of degrees of freedom of local problems.

Since the DtN map is inconvenient for numerical computation due to its non-local property, it is required to approximate the DtN map in terms of local operators. To this end there have been many approaches such as Talyor approximations [12] and first and second order optimized methods [1, 2, 4]. In this paper, we utilize complete radiation boundary conditions [13, 14] for its approximation. This can be done in that not only can CRBCs be thought of as approximate operators to DtN map but they can also be imposed with Neumann data coming from neighboring subdomains as the output of the neighbor's DtN map on the interfaces between neighboring subdomains. Here CRBCs are high-order absorbing boundary conditions designed to approximate the exact radiation condition for numerical computations. They are developed based on the Higdon's high order absorbing boundary conditions [15, 16] and are modified to be more suitable for numerical applications by introducing auxiliary functions satisfying certain three term recurrence relations with some parameters. It is also shown that these damping parameters of CRBCs can be easily tuned optimally for minimizing reflections from artificial boundaries.

We note that our optimized double sweep Schwarz method is related to that of [10] involving nonoverlapping subdomains with Neumann data. However the algorithm in [10] produces discontinuous solutions while our method leads to continuous ones and hence well suited for a preconditioner of Krylov space methods for the full problem such as GMRES. It can also be found that [11] utilizes the DtN map for the transparent boundary condition in their double sweep process. Their double sweep process serves as a preconditioner for the parallel Schwarz method, but our paper studies the pure double sweep Schwarz method to handle the case where one end is closed as the model problem. Furthermore, we will provide the analysis showing that our optimized double sweep Schwarz formulation with the approximate transparent condition imposed on the interfaces of subdomains, combined with the convergence of solutions satisfying CRBCs to radiating solutions investigated in [13], gives rise to the convergence result of the proposed domain decomposition algorithm.

At last, it can be found in [5] that CRBCs have been used successfully for transmission conditions of a nonoverlapping Schwarz method, which is examined as Jacobi-type GMRES preconditioners. The sweeping algorithm in this paper can be considered as Gauss-Seidel preconditioning for GMRES implementations, which is more appropriate for the model problems under consideration due to reflection from the cavity part. Also, we notice that from a computational point of view implementing the algorithm based on Neumann data in this paper is simpler and more stable than that in [5], where subdomain problems exchange information via auxiliary functions of CRBCs.

The outline of the reminder of the paper is given as follows. Section 2 presents preliminaries such as notations and basic Sobolev spaces to be used throughout the paper and we review well-posedness of subdomain problems associated with the exact radiation condition. As the essential idea of our analysis, transferring Neumann data in the forward sweeping step is discussed in Section 3. Section 4 provides the analysis of the backward sweeping step to construct full wave expansions. Section 5 is devoted to introducing CRBCs as an approximate operator to the DtN map and reviewing their equivalent formulas and the convergence result. It also presents an approximate algorithm of the above steps introduced in Section 3 and 4 by replacing the exact DtN map with CRBCs and we study convergence of the new optimized double sweep Schwarz method with CRBCs. In Section 6 we discuss about implementation of the optimized double sweep Schwarz method. Finally, Section 7 reports the results of numerical examples illustrating the convergence behavior of approximate solutions of our method.

2. Preliminaries

With a sequence of real numbers $0 = b_0 < b_1 < \ldots < b_L = b$, we decompose the domain Ω into the subregions

$$\Omega_j = (b_{j-1}, b_j) \times \Theta \text{ for } j = 1, \ldots, L-1,$$
$$\Omega_L = \Omega_\infty \cap \{(x, y) \in \mathbb{R} \times \mathbb{R}^{d-1} \ : \ x > b_{L-1}\}$$

with $\Gamma_j = \{b_j\} \times \Theta$. See Figure 1. Also, we define $\Omega_{i,j} = (b_i, b_j) \times \Theta$ for $0 \le i < j \le L$. Here we assume that $\beta = b_j - b_{j-1}$ is constant for $j = 1, 2, \ldots, L$ for notational simplicity.

Let $\{Y_n\}_{n=0}^{\infty}$ be the orthonormal basis of $L^2(\Theta)$ consisting of eigenvectors for the transversal negative Laplace operator in Θ satisfying

$$-\Delta_y Y_n = \lambda_n^2 Y_n \text{ in } \Theta,$$
$$\frac{\partial Y_n}{\partial \nu} = 0 \text{ on } \partial\Theta.$$

Here λ_n^2 for $n = 0, 1, \ldots$ represent eigenvalues associated with eigenvectors Y_n and satisfy

$$\lambda_n^2 \sim C n^{\frac{2}{d-1}} \tag{2.1}$$

asymptotically for large n with some positive constant C, see e.g., [17, Ch. VI, Theorem 20,21]. We define a Sobolev space $H^s(\Theta)$ for $s \in \mathbb{R}$ on the cross section Θ by the set of all functions $\phi = \sum_{n=0}^{\infty} \phi_n Y_n$ such that

$$\|\phi\|_{H^s(\Theta)}^2 = \sum_{n=0}^{\infty} (1 + \lambda_n^2)^s |\phi_n|^2$$

is bounded.

By identifying Γ_0 with Θ and defining $\mu_n^2 = k^2 - \lambda_n^2$ for $n = 0, 1, \ldots$, the DtN operator $T : H^{1/2}(\Theta) \to H^{-1/2}(\Theta)$ is defined by

$$T(u) = \sum_{n=0}^{\infty} i\mu_n u_n Y_n$$

for $u = \sum_{n=0}^{\infty} u_n Y_n$ in $H^{1/2}(\Theta)$.

Since the radiating solution in Ω_∞ can be written as the Fourier series

$$u(x,y) = \sum_{n=0}^{\infty} B_n e^{-i\mu_n x} Y_n(y) \tag{2.2}$$

about Γ_0 for some constants B_n, the boundary condition based on the DtN operator on Γ_0 is the exact radiation condition for the truncated problem. Also, it is well-known that the problem (1.1) has a unique solution provided that k^2 is not a Neumann eigenvalue of the problem (1.1) in the semi-infinite waveguide, see e.g., [18]. From here on, we assume that k^2 is not a Neumann eigenvalue of the semi-infinite waveguide Ω_∞ for the well-posedness of the problem. On the other hand, as we will develop a domain decomposition technique in the setting of one-way domain splitting along the x-axis, the well-posedness of local wave propagation problems is required as well. For this reason, we further assume that there is no cutoff frequency, i,e., $k^2 \neq \lambda_n^2$ for $n = 0, 1, \ldots$. It is noted in [19] that the Helmholtz equation posed in the straight waveguide $(a_0, a_1) \times \Theta$ for any real $a_0 < a_1$ with the DtN transparent boundary condition at $x = a_0, a_1$ is well-posed except for $k^2 = \lambda_n^2$ and modes corresponding to the cutoff frequencies are eigenfunctions. Under this situation, there exists an integer $N > 0$ such that

$$k^2 > \lambda_N^2 \quad \text{and } k^2 < \lambda_{N+1}^2$$

and so the radiation solution u given by (2.2) can be interpreted as a superposition of propagating modes and evanescent modes

$$u(x,y) = \sum_{n=0}^{N} B_n e^{-i\mu_n x} Y_n(y) + \sum_{n=N+1}^{\infty} B_n e^{\tilde{\mu}_n x} Y_n(y) \text{ for } x < 0,$$

where $\tilde{\mu}_n = \sqrt{\lambda_n^2 - k^2} > 0$ for $n > N$.

For the variational representation of the model problem, we let $H^1(D)$ for domains D in $\mathbb{R}^d$ represent a standard Sobolev space of L^2-integrable functions defined in D together with their first derivatives. By $\widetilde{L}^2(D)$ we denote a subset of $L^2(D)$ consisting of compactly supported functions. Let $(\cdot,\cdot)_D$ and $\langle \cdot,\cdot \rangle_{\Gamma_j}$ be the L^2-inner product in D and the duality pairing between $H^{-1/2}(\Gamma_j)$ and $H^{1/2}(\Gamma_j)$, respectively. We introduce the sesquilinear form $\mathcal{A}(\cdot,\cdot)$ defined by

$$\mathcal{A}(u,v) = (\nabla u, \nabla v)_\Omega - k^2 (u,v)_\Omega - \langle Tu, v\rangle_{\Gamma_0} \text{ for } u, v \in H^1(\Omega).$$

Then the the problem (1.1) is reformulated in a variational form to find $u \in H^1(\Omega)$ satisfying

$$\mathcal{A}(u,\phi) = (-f, \phi)_\Omega \text{ for } \phi \in H^1(\Omega).$$

Assume that $f = \sum_{j=1}^{L} f_j$ such that f_j belongs to $\widetilde{L}^2(\Omega_j)$. Due to the linearity of the problem, the solution u to the problem (1.1) can be written as a superposition of solutions resulting from each source f_j, i.e., $u = \sum_{j=1}^{L} u_j$, where u_j is the solution to the problem

$$\mathcal{A}(u_j,\phi) = (-f_j, \phi)_\Omega \text{ for } \phi \in H^1(\Omega). \tag{2.3}$$

We now discuss the well-posedness of the problem posed in a straight waveguide $D = (a, b) \times \Theta$ for any real $a < b$ with the left boundary $\Gamma_a = \{a\} \times \Theta$ and the right boundary $\Gamma_b = \{b\} \times \Theta$. In particular, for $f \in \widetilde{L}^2(D)$, $g_N \in H^{-1/2}(\Gamma_a)$ and $g_D \in H^{1/2}(\Gamma_b)$, the well-posedness of wave propagation problems with Neumann data (2.4) or with Dirichlet-Neumann data (2.5) is presented,

$$\begin{aligned} &\Delta u + k^2 u = f \text{ in } D, \\ &\qquad \frac{\partial u}{\partial \nu} = T(u) + g_N \text{ on } \Gamma_a \quad \text{and} \quad \frac{\partial u}{\partial \nu} = T(u) \text{ on } \Gamma_b \end{aligned} \tag{2.4}$$

and

$$\begin{aligned} &\Delta u + k^2 u = f \text{ in } D, \\ &\qquad \frac{\partial u}{\partial \nu} = T(u) + g_N \text{ on } \Gamma_a \quad \text{and } u = g_D \text{ on } \Gamma_b, \end{aligned} \tag{2.5}$$

with the sound-hard boundary condition $\partial u / \partial \nu = 0$ on $(a, b) \times \partial \Theta$, respectively. From now on, we assume that the sound-hard boundary condition is imposed on physical boundaries unless otherwise stated. These problems will serve as local problems of the double sweep Schwarz algorithm proposed in this paper. The following lemmas are standard and they can be proved by invoking the Fredholm alternative and so their proofs are omitted.

Lemma 2.1. *The problem* (2.4) *has a unique solution u in $H^1(D)$. In addition, it holds that*

$$\|u\|_{H^1(D)} \le C(\|f\|_{L^2(D)} + \|g_N\|_{H^{-1/2}(\Gamma_a)}).$$

Lemma 2.2. *The problem* (2.5) *has a unique solution u in $H^1(D)$. In addition, it holds that*

$$\|u\|_{H^1(D)} \le C(\|f\|_{L^2(D)} + \|g_N\|_{H^{-1/2}(\Gamma_b)} + \|g_D\|_{H^{1/2}(\Gamma_a)}).$$

At last, we address the regularity result for solutions to the local wave propagation problems investigated in [20, 18].

Remark 2.3. *The regularity of solutions u to the problem* (2.4) *with $g_N \in H^{1/2}(\Gamma_a)$ is*

$$\|u\|_{H^2(D)} \le C(\|f\|_{L^2(D)} + \|g_N\|_{H^{1/2}(\Gamma_a)}).$$

3. Data transferring via the exact DtN operator

Let $1 \le j \le L - 1$ and $\hat{f} \in \widetilde{L}^2(\Omega_{0,j})$. Now we consider the problem

$$\mathcal{A}(\hat{u}, \phi) = (-\hat{f}, \phi)_\Omega \text{ for } \phi \in H^1(\Omega). \tag{3.1}$$

The wave expansion of the solution $\hat{u}$ restricted to $\Omega_{j,L}$ consists of the right-going modes and left-going modes,

$$\begin{aligned} \hat{u}(x, y) &= \sum_{n=0}^{\infty} A_n e^{i\mu_n x} Y_n(y) + \sum_{n=0}^{\infty} B_n e^{-i\mu_n x} Y_n(y) \\ &:= u_r(x, y) + u_l(x, y) \quad \text{ in } \Omega_{j,L}. \end{aligned} \tag{3.2}$$

In order to examine $\hat{u}$ in more detail, let $\tilde{u}_r$ be the radiating solution of the problem with the same source $\hat{f}$ but in the straight waveguide $\Omega_{0,L}$,

$$\begin{aligned} \Delta\tilde{u}_r + k^2\tilde{u}_r &= \hat{f} \text{ in } \Omega_{0,L}, \\ \frac{\partial \tilde{u}_r}{\partial \nu} &= T(\tilde{u}_r) \text{ on } \Gamma_0 \cup \Gamma_L, \end{aligned} \tag{3.3}$$

where ν is the outward unit normal vector on the boundary of $\Omega_{0,L}$. Sometimes, we will use $\nu_{i,j}$ for the unit normal vector on the common boundary from Ω_i to Ω_j.

Now we consider the total wave field $\tilde{u}_l$ generated when $\tilde{u}_r$ propagates into the cavity $\Omega_{j,L} \cup \Omega_L$ through Γ_j. We know that $\tilde{u}_l$ in $\Omega_{j,L}$ is also decomposed into outgoing (left-going) and incoming (right-going) components as in (3.2), which are denoted by $\tilde{u}_l^{out}$ and $\tilde{u}_l^{in}$, respectively, i.e., $\tilde{u}_l = \tilde{u}_l^{out} + \tilde{u}_l^{in}$ in $\Omega_{j,L}$. Since there is no incoming wave source except for $\tilde{u}_r$, it is clear that $\tilde{u}_l^{in} = \tilde{u}_r$ in $\Omega_{j,L}$. Noting that $\tilde{u}_r$ represents the right-going wave in $\Omega_{j,L}$, it follows that on Γ_j with $\nu = \nu_{j+1,j}$

$$\begin{aligned} \frac{\partial \tilde{u}_l}{\partial \nu} &= \frac{\partial \tilde{u}_l^{out}}{\partial \nu} + \frac{\partial \tilde{u}_l^{in}}{\partial \nu} = T(\tilde{u}_l^{out}) - T(\tilde{u}_r) \\ &= T(\tilde{u}_l) - 2T(\tilde{u}_r) = T(\tilde{u}_l) + 2\frac{\partial \tilde{u}_r}{\partial \nu}. \end{aligned} \tag{3.4}$$

Therefore, $\tilde{u}_l$ is the solution to the problem in $\Omega_{j,L} \cup \Omega_L$

$$\begin{aligned} \Delta\tilde{u}_l + k^2\tilde{u}_l &= 0 \text{ in } \Omega_{j,L} \cup \Omega_L, \\ \frac{\partial \tilde{u}_l}{\partial \nu} &= T(\tilde{u}_l) + 2\frac{\partial \tilde{u}_r}{\partial \nu} \text{ on } \Gamma_j. \end{aligned}$$

In the following lemma, we can show that the right-going component u_r of $\hat{u}$ in $\Omega_{j,L}$ is identified with the right-going one generated solely by the wave source $\hat{f}$ in the straight waveguide, in other words, $u_r = \tilde{u}_r$ in $\Omega_{j,L}$ and the left-going component u_l of $\hat{u}$ in $\Omega_{j,L}$ is one that results from the reflection of the propagation of u_r into $\Omega_{j,L} \cup \Omega_L$, i.e., $u_l = \tilde{u}_l^{out}$ in $\Omega_{j,L}$.

Lemma 3.1. *Assume that $\hat{u}$, $\tilde{u}_r$, $\tilde{u}_l$ and $\tilde{u}_l^{out}$ are defined as above. Then it holds that*

(1) $\hat{u} = \tilde{u}_r + \tilde{u}_l^{out}$ in the straight waveguide $\Omega_{0,L}$,
(2) $\hat{u} = \tilde{u}_l$ in $\Omega_{j,L} \cup \Omega_L$.

PROOF. We first extend the left-going component $\tilde{u}_l^{out}$ to $\Omega_{0,j}$ by taking the solution to the problem

$$\begin{aligned} \Delta\phi + k^2\phi &= 0 \text{ in } \Omega_{0,j}, \\ \frac{\partial \phi}{\partial \nu} &= T(\phi) \text{ on } \Gamma_0 \text{ and } \phi = \tilde{u}_l^{out} \text{ on } \Gamma_j. \end{aligned}$$

By considering $\tilde{u}_l^{out}$ as the extended function defined in $\Omega_{0,L}$, we define

$$v(x,y) = \begin{cases} \tilde{u}_r(x,y) + \tilde{u}_l^{out}(x,y) & \text{for } (x,y) \in \Omega_{0,L}, \\ \tilde{u}_l(x,y) & \text{for } (x,y) \in \Omega_{j,L} \cup \Omega_L. \end{cases}$$

Since $\tilde{u}_r + \tilde{u}_l^{out}$ coincides with $\tilde{u}_l$ in the transition layer $\Omega_{j,L}$ by the definition of $\tilde{u}_r, \tilde{u}_l^{out}$ and $\tilde{u}_l$, v is well-defined. Clearly, v is the solution to the problem (3.1), which leads to (1) and (2).

Now, we will discuss the right sweeping algorithm in which data of the right-going component generated by f_j in Ω_j are transferred to the right neighboring domain Ω_{j+1} as incoming data. Let $w_0 = 0$. For $j = 1, \ldots, L$, with a given right-going component of w_{j-1} near Γ_{j-1} in Ω_{j-1} as incoming data, we solve the problem with the source f_j in the straight waveguide $\Omega_{j-1,L}$ to find w_j satisfying

$$\begin{aligned} &\Delta w_j + k^2 w_j = f_j \text{ in } \Omega_{j-1,L}, \\ &\qquad \frac{\partial w_j}{\partial \nu} = T(w_j) + g_{j-1} \text{ on } \Gamma_{j-1} \text{ and } \frac{\partial w_j}{\partial \nu} = T(w_j) \text{ on } \Gamma_L, \end{aligned} \tag{3.5}$$

where $g_{j-1} = 2\partial w_{j-1}/\partial \nu_{j,j-1}$ on Γ_{j-1} is the incoming data.

Lemma 3.2. *For $1 \le j \le L-1$, let v_j be the solution to the problem* (3.3) *for $\hat{f} := \sum_{\ell=1}^{j} f_j$. Then it holds that $v_j = w_j$ in $\Omega_{j-1,L}$.*

Proof. When $j = 1$, since v_1 solves the same equation as w_1, it is obvious that $v_1 = w_1$ in $\Omega_{0,L}$.

Assume that $v_{j-1} = w_{j-1}$ in $\Omega_{j-2,L}$ for $2 \le j \le L-1$. Now, we see that v_j is a superposition of two wave fields, $v_j = v_{j-1} + \tilde{v}_j$, one of which is v_{j-1} resulting from the source $\sum_{\ell=1}^{j-1} f_j$ and the other denoted by $\tilde{v}_j$ is generated by f_j, i.e., $\tilde{v}_j$ is the radiating solution to the problem

$$\begin{aligned} &\Delta \tilde{v}_j + k^2 \tilde{v}_j = f_j \text{ in } \Omega_{j-1,L}, \\ &\qquad \frac{\partial \tilde{v}_j}{\partial \nu} = T(\tilde{v}_j) \text{ on } \Gamma_{j-1} \cup \Gamma_L. \end{aligned} \tag{3.6}$$

By the inductive assumption, it holds that $v_{j-1} = w_{j-1}$ in $\Omega_{j-2,L}$ and hence v_{j-1} satisfies the equations

$$\begin{aligned} &\Delta v_{j-1} + k^2 v_{j-1} = 0 \text{ in } \Omega_{j-1,L}, \\ &\qquad \frac{\partial v_{j-1}}{\partial \nu} = T(v_{j-1}) + g_{j-1} \text{ on } \Gamma_{j-1} \text{ and } \frac{\partial v_{j-1}}{\partial \nu} = T(v_{j-1}) \text{ on } \Gamma_L. \end{aligned} \tag{3.7}$$

From the linearity of the problems (3.6) and (3.7), it follows that $v_j = v_{j-1} + \tilde{v}_j$ is the solution to the problem (3.5) and hence $v_j = w_j$ in $\Omega_{j-1,L}$, which completes the proof by the induction argument.

We are interested in finding data g_{j-1} coming into Ω_j, which can be achieved by solving the problem (3.5) and taking $g_j = 2\partial w_j/\partial\nu_{j+1,j}$ for $j = 1, 2, \ldots, L-1$ with $g_0 = 0$. However, we can do this by solving problems in smaller domains Ω_j instead of problems (3.5) in larger domains $\Omega_{j-1,L}$. In fact, the solution (restricted to Ω_j) to the wave propagation problem (3.5) in the straight waveguide $\Omega_{j-1,L}$ is identical with one to the problem in Ω_j,

$$\begin{aligned} &\Delta\tilde{w}_j + k^2\tilde{w}_j = f_j \text{ in } \Omega_j, \\ &\qquad \frac{\partial\tilde{w}_j}{\partial\nu} = T(\tilde{w}_j) + \tilde{g}_{j-1} \text{ on } \Gamma_{j-1} \text{ and } \frac{\partial\tilde{w}_j}{\partial\nu} = T(\tilde{w}_j) \text{ on } \Gamma_j, \end{aligned} \tag{3.8}$$

where $\tilde{g}_{j-1} = 2\partial\tilde{w}_{j-1}/\partial\nu_{j,j-1}$ on Γ_{j-1} with $\tilde{g}_0 = 0$.

Lemma 3.3. *Let w_j and $\tilde{w}_j$ be the solutions to the problem* (3.5) *and* (3.8)*, respectively. Then w_j restricted to Ω_j coincides with $\tilde{w}_j$ in Ω_j. In addition, $g_{j-1} = \tilde{g}_{j-1}$ on Γ_{j-1} for $j = 1, 2, \ldots, L$.*

Proof. This is due to the fact that the boundary conditions based on the DtN operator on Γ_L in (3.5) and Γ_j in (3.8) are the exact radiation boundary condition. The solution of (3.5) ((3.8), respectively) is considered as the restriction to $\Omega_{j-1,L}$ (Ω_j, respectively) of the solution to the semi-infinite waveguide problem in $(b_{j-1}, \infty) \times \Theta$ satisfying the radiation condition. Since the initial incoming data g_0 and $\tilde{g}_0$ are equal, the induction argument completes the proof.

We construct inductively the Neumann incoming data $\tilde{g}_{j-1}$ coming into the domain Ω_j for $j = 1, 2, \ldots, L$ with $\tilde{g}_0 = 0$ by solving local problems (3.8).

Algorithm 1. Right sweeping to find the incoming data $\tilde{g}_j = 2\partial\tilde{w}_j/\partial\nu_{j+1,j}$ for $j = 1, 2, \ldots, L-1$:

1. *Set $\tilde{g}_0 = 0$.*
2. *Do for $j = 1, 2, \ldots, L-1$,*
    - *i. Solve* (3.8) *for $\tilde{w}_j$.*
    - *ii. Compute $\tilde{g}_j = 2\dfrac{\partial\tilde{w}_j}{\partial\nu_{j+1,j}} = -2\dfrac{\partial\tilde{w}_j}{\partial x}$ on Γ_j.*

    End do

We close this section with the following regularity result for solutions to the local wave propagating problem mentioned in Remark 2.3.

Remark 3.4. *As a consequence of Lemma 3.2, Lemma 3.3 and the regularity of solutions to the problem* (3.3)*, we have*

$$\|\tilde{w}_j\|_{H^2(\Omega_j)} \leq C\|\sum_{\ell=1}^{j} f_\ell\|_{L^2(\Omega)}.$$

4. Full wave expansion

In this section, we shall find the wave expansion of the solution u in each subregion Ω_j for $j = 1, 2, \ldots, L$. During the backward sweep, we solve the subdomain problems with the transparent condition on the left boundary and the Dirichlet condition on the right boundary. Here it is worth pointing out that any condition on the right boundary that makes the local problem well-posed can be used for the optimal convergence (see e.g., [21]). Here we choose the Dirichlet condition on the right boundary of each subdomain for the continuity of the approximate solution on the interfaces. The Dirichlet condition is important to get continuous iterates across the nonoverlapping subdomains for our analysis at the PDE level.

Assuming that $\tilde{g}_j$ for $0 \le j \le L-1$ are determined by *Algorithm 1*, we begin with finding the solution u restricted to Ω_L to the problem (1.1). Let $\tilde{w}_L$ be the function satisfying

$$\begin{aligned} \Delta \tilde{w}_L + k^2 \tilde{w}_L &= f_L \text{ in } \Omega_L, \\ \frac{\partial \tilde{w}_L}{\partial \nu} &= T(\tilde{w}_L) + \tilde{g}_{L-1} \text{ on } \Gamma_{L-1}. \end{aligned} \tag{4.1}$$

Theorem 4.1. *Let u and $\tilde{w}_L$ be the solutions to the problem* (1.1) *and* (4.1)*, respectively. Then $u = \tilde{w}_L$ in Ω_L.*

Proof. By the linearity of the problem, u can be decomposed into $u = u_L + \hat{u}_L$, where u_L and $\hat{u}_L$ are the solutions to the problems

$$\mathcal{A}(u_L, \phi) = (-f_L, \phi)_\Omega \text{ for } \phi \in H^1(\Omega)$$

and

$$\mathcal{A}(\hat{u}_L, \phi) = (-\hat{f}, \phi)_\Omega \text{ for } \phi \in H^1(\Omega),$$

respectively, where $\hat{f} = \sum_{\ell=1}^{L-1} f_j$.

We first note that the radiating solution u_L solves the problem

$$\begin{aligned} \Delta u_L + k^2 u_L &= f_L \text{ in } \Omega_L, \\ \frac{\partial u_L}{\partial \nu} &= T(u_L) \text{ on } \Gamma_{L-1}. \end{aligned} \tag{4.2}$$

On the other hand, let w_{L-1} be the solution to the problem (3.5) with $j = L-1$. Lemma 3.2 shows that w_{L-1} about Γ_{L-1} is the right-going wave field generated by $\hat{f}$, and then it follows from Lemma 3.1 that $\hat{u}_L$ solves the problem

$$\begin{aligned} \Delta \hat{u}_L + k^2 \hat{u}_L &= 0 \text{ in } \Omega_L, \\ \frac{\partial \hat{u}_L}{\partial \nu} &= T(\hat{u}_L) + \tilde{g}_{L-1} \text{ on } \Gamma_{L-1}, \end{aligned} \tag{4.3}$$

where $\tilde{g}_{L-1} = 2\partial w_{L-1}/\partial \nu_{L,L-1}$ on Γ_{L-1}. Combining (4.2) and (4.3) implies that $u = w_L$ in Ω_L.

For $\tilde{g}_j$ with $j = 0, 1, \ldots, L-1$ determined by *Algorithm 1* and $\tilde{w}_L (= u)$ in Ω_L obtained by solving the problem (4.1), we shall find the solution u in each domain Ω_j inductively from $j = L-1$ to $j = 1$ as follows. Setting $z_L = \tilde{w}_L$ and assuming that z_{j+1} is given in Ω_{j+1} for $j < L$, we find the unique solution z_j in Ω_j to the problem

$$\begin{aligned} \Delta z_j + k^2 z_j &= f_j \text{ in } \Omega_j, \\ \frac{\partial z_j}{\partial \nu} &= T(z_j) + \tilde{g}_{j-1} \text{ on } \Gamma_{j-1} \quad \text{and} \quad z_j = z_{j+1} \text{ on } \Gamma_j. \end{aligned} \tag{4.4}$$

Theorem 4.2. *Let u be the solution to the problem* (1.1) *and let z_j be defined as above for $j = L, L-1, \ldots, 1$. Then we have $z_j = u$ in Ω_j for $j = L, L-1, \ldots, 1$.*

Proof. By the definition of z_L and Theorem 4.1, we have $z_L = u$ in Ω_L. We will first show that $z_j = u$ in Ω_j under the assumption that $z_{j+1} = u$ in Ω_{j+1} for $1 \leq j < L$.

The proof proceeds by splitting the solution u into two wave fields, $u = \hat{u}_1 + \hat{u}_2$, where $\hat{u}_j$ for $j = 1, 2$ is the solution to the problem

$$\mathcal{A}(\hat{u}_j, \phi) = (-\hat{f}_j, \phi)_\Omega \text{ for } \phi \in H^1(\Omega),$$

with $\hat{f}_1 = \sum_{\ell=1}^{j} f_\ell$ and $\hat{f}_2 = \sum_{\ell=j+1}^{L} f_\ell$.

Now, by Lemma 3.1 the first wave field $\hat{u}_1$ can be also decomposed into two parts, $\hat{u}_1 = \tilde{u}_r + \tilde{u}_l^{out}$ in $\Omega_{0,L}$, where $\tilde{u}_r$ and $\tilde{u}_l^{out}$ are defined as in Lemma 3.1, and hence

$$u = \tilde{u}_r + \tilde{u}_l^{out} + \hat{u}_2 \text{ in } \Omega_{0,L}. \tag{4.5}$$

By Lemma 3.2 and Lemma 3.3, we can show that $\tilde{u}_r$ is the solution to the problem

$$\begin{aligned} \Delta \tilde{u}_r + k^2 \tilde{u}_r &= f_j \text{ in } \Omega_j, \\ \frac{\partial \tilde{u}_r}{\partial \nu} &= T(\tilde{u}_r) + \tilde{g}_{j-1} \text{ on } \Gamma_{j-1} \quad \text{and} \quad \frac{\partial \tilde{u}_r}{\partial \nu} = T(\tilde{u}_r) \text{ on } \Gamma_j. \end{aligned} \tag{4.6}$$

By using (4.5) and the fact that $z_{j+1} = u$ on Γ_j and $\tilde{u}_l^{out} + \hat{u}_2$ satisfies the radiation condition on Γ_{j-1}, it is easy to see that $\tilde{u}_l^{out} + \hat{u}_2$ satisfies

$$\begin{aligned} (\Delta + k^2)(\tilde{u}_l^{out} + \hat{u}_2) &= 0 \text{ in } \Omega_j, \\ \frac{\partial}{\partial \nu}(\tilde{u}_l^{out} + \hat{u}_2) &= T((\tilde{u}_l^{out} + \hat{u}_2)) \text{ on } \Gamma_{j-1}, \\ (\tilde{u}_l^{out} + \hat{u}_2) &= z_{j+1} - \tilde{u}_r \text{ on } \Gamma_j. \end{aligned} \tag{4.7}$$

Finally, adding the solutions to two problems (4.6) and (4.7), we see that $u = \tilde{u}_r + \tilde{u}_l^{out} + \hat{u}_2$ in Ω_j is the unique solution to the problem (4.4), which implies that $z_j = u$ in Ω_j.

Now, we are in the position to describe the algorithm to construct local solutions in Ω_j, which coincide with the solution u to the problem (1.1) in Ω_j.

Assume that we have the incoming data $\tilde{g}_j$ for $j = 0, 1, \ldots, L-1$ by *Algorithm 1.*

Algorithm 2. Left sweeping to find the wave expansion z_j in Ω_j for $j = L, L-1, \ldots, 1$:

1. *Find z_L by solving the problem* (4.1) *in Ω_L.*
2. *Do for $j = L-1, \ldots, 1$,*
   i. Compute the Dirichlet data of z_{j+1} on Γ_j.
   ii. Find z_j by solving the problem (4.4) *in Ω_j.*
   End do

5. Approximate wave expansion with complete radiation boundary conditions

This section is devoted to introducing the optimized double sweep Schwarz algorithm with the exact DtN map replaced by high-order approximate radiation conditions, so-called complete radiation boundary conditions. By employing CRBCs, the local problems can be easily discretized with sparse linear systems.

5.1. Complete radiation boundary conditions

The complete radiation boundary conditions have been developed to approximate the exact radiation condition based on the DtN operator $T : H^{1/2}(\Theta) \to H^{-1/2}(\Theta)$. In order to define CRBCs, we need distinct damping parameters given as follows: let n_p and n_e be non-negative integers determining the order (n_p, n_e) of CRBCs,

$$a_j = \begin{cases} -ikc_j & \text{for } j = 0, 1, \ldots, n_p - 1, \\ \sigma_j & \text{for } j = n_p, \ldots, n_p + n_e - 1 \end{cases} \tag{5.1}$$

and

$$\tilde{a}_j = \begin{cases} -ik\tilde{c}_j & \text{for } j = 0, 1, \ldots, n_p - 1, \\ \tilde{\sigma}_j & \text{for } j = n_p, \ldots, n_p + n_e - 1 \end{cases} \tag{5.2}$$

with the conditions

$$\mu_{min}/k \le c_j, \tilde{c}_j \le 1 \text{ and } \tilde{\mu}_{min} \le \sigma_j, \tilde{\sigma}_j \le \tilde{\mu}_{max}. \tag{5.3}$$

Here μ_{min} and $\tilde{\mu}_{min}$ are the smallest axial frequency of propagating modes and the smallest decay rate of evanescent modes, respectively. For instance, $\mu_{min} = \mu_N$ and $\tilde{\mu}_{min} = \tilde{\mu}_{N+1}$ in the model problem. Also, $\tilde{\mu}_{max}$ denotes an upper bound of the axial frequencies of evanescent modes that numerical techniques depending on mesh size h can support.

The CRBC on Γ_0 for the radiation condition for $x \to -\infty$ is defined in terms of auxiliary functions ϕ_j defined in $(0, \delta) \times \Theta$ for small constant $\delta > 0$ as follows: there exist ϕ_j for $j = 0, 1, \ldots, n_p + n_e$ satisfying the Helmholtz equation

$\Delta\phi_j + k^2\phi_j = 0$ in $(0,\delta)\times\Theta$ with $\partial\phi_j/\partial\nu = 0$ on $(0,\delta)\times\partial\Theta$ and the recurrence relations

$$\phi_0 = u \text{ in } (0,\delta)\times\Theta,$$
$$(\frac{\partial}{\partial\nu} + a_j)\phi_j = (-\frac{\partial}{\partial\nu} + \tilde{a}_j)\phi_{j+1} \text{ in } (0,\delta)\times\Theta \tag{5.4}$$

($\partial/\partial\nu = -\partial/\partial x$ is the outward normal derivative with respect to the boundary Γ_0) for $j = 0, 1, \ldots, n_p + n_e - 1$ with the terminal condition

$$\frac{\partial}{\partial\nu}\phi_{n_p+n_e} = 0 \text{ on } \Gamma_0. \tag{5.5}$$

Here let $P = n_p + n_e - 1$.

Since auxiliary functions ϕ_j satisfy the Helmholtz equation, they can be written as the series

$$\phi_j(x,y) = \sum_{n=0}^{\infty}(A_n^j e^{i\mu_n x} + B_n^j e^{-i\mu_n x})Y_n(y) \text{ in } (0,\delta)\times\Theta.$$

Noting that the solution u is also written as

$$u(x,y) = \sum_{n=0}^{\infty}(A_n e^{i\mu_n x} + B_n e^{-i\mu_n x})Y_n(y) \text{ in } (0,\delta)\times\Theta$$

with $A_n^0 = A_n$ and $B_n^0 = B_n$, the recurrence relations (5.4) reveal that Fourier coefficients A_n^j and B_n^j of ϕ_j satisfy

$$(a_j - i\mu_n)A_n^j = (\tilde{a}_j + i\mu_n)A_n^{j+1} \quad \text{and} \quad (a_j + i\mu_n)B_n^j = (\tilde{a}_j - i\mu_n)B_n^{j+1}$$

for $j = 0, 1, \ldots, P$. Therefore, if a damping parameter $\tilde{a}_j$ is chosen so that $\tilde{a}_j = -i\mu_n$ for some n, then we can see that $A_n = A_n^1 = \ldots = A_n^j = 0$ and the CRBC behaves as the exact radiation condition for the n-th modes. Otherwise, since

$$A_n^{P+1} = \left(\prod_{j=0}^{P}\frac{a_j - i\mu_n}{\tilde{a}_j + i\mu_n}\right)A_n \quad \text{and} \quad B_n^{P+1} = \left(\prod_{j=0}^{P}\frac{a_j + i\mu_n}{\tilde{a}_j - i\mu_n}\right)B_n,$$

the terminal condition (5.5) leads to

$$A_n = \prod_{j=0}^{P}\frac{(a_j + i\mu_n)(\tilde{a}_j + i\mu_n)}{(a_j - i\mu_n)(\tilde{a}_j - i\mu_n)}B_n,$$

which shows that the reflection coefficient for the n-th modes is given by

$$\rho = \prod_{j=0}^{P}\left|\frac{(a_j + i\mu_n)(\tilde{a}_j + i\mu_n)}{(a_j - i\mu_n)(\tilde{a}_j - i\mu_n)}\right|.$$

Due to the definitions (5.1) and (5.2) of the parameters and the conditions (5.3), it is clear that

$$\left|\frac{(a_j + i\mu_n)(\tilde{a}_j + i\mu_n)}{(a_j - i\mu_n)(\tilde{a}_j - i\mu_n)}\right| < 1 \begin{cases} \text{for } j = 0, 1, \ldots, n_p - 1 & \text{if } n \le N, \\ \text{for } j = n_p, \ldots, n_p + n_e - 1 & \text{if } n > N, \end{cases}$$

which shows that reflection coefficients for important modes can be reduced exponentially by increasing parameters. More precisely, it is shown in [22] that by solving the min-max problems

$$\rho_p \equiv \min_{\substack{a_0,\ldots,a_{n_p-1},\\ \tilde{a}_0,\ldots,\tilde{a}_{n_p-1}\in i\mathbb{R}_-}} \max_{\mu\in[\mu_{min},k]} \prod_{j=0}^{n_p-1} \left|\frac{(a_j + i\mu)(\tilde{a}_j + i\mu)}{(a_j - i\mu)(\tilde{a}_j - i\mu)}\right|, \tag{5.6}$$

$$\rho_e \equiv \min_{\substack{a_{n_p},\ldots,a_{n_p+n_e-1}\\ \tilde{a}_{n_p},\ldots,\tilde{a}_{n_p+n_e-1}\in\mathbb{R}_+}} \max_{\mu\in[\tilde{\mu}_{min},\tilde{\mu}_{max}]} \prod_{j=n_p}^{n_p+n_e-1} \left|\frac{(a_j - \mu)(\tilde{a}_j - \mu)}{(a_j + \mu)(\tilde{a}_j + \mu)}\right|, \tag{5.7}$$

the reflection coefficients ρ_p and ρ_e for propagating modes and evanescent modes satisfy

$$\rho_p \le e^{-Cn_p/\ln(k/\mu_{min})} \quad\text{and}\quad \rho_e \le e^{-Cn_e/\ln(\tilde{\mu}_{max}/\tilde{\mu}_{min})}.$$

See [5] to find examples showing how the parameters a_j and $\tilde{a}_j$ for given k and CRBC order (n_p, n_e) are distributed and how the reflection coefficients behaves for each important modes.

The CRBCs defined by the recurrence relations (5.4)-(5.5) of auxiliary functions can be interpreted as an approximate DtN operator. In [13], it is shown that CRBCs are equivalent to the boundary condition associated with the operator $T_{tc} : H^{1/2}(\Gamma_0) \to H^{-1/2}(\Gamma_0)$ defined by

$$T_{tc}(u) = \sum_{n=0}^{\infty} i\mu_n \frac{1 - Z^n_{0,P}}{1 + Z^n_{0,P}} u_n Y_n \tag{5.8}$$

for $u = \sum_{n=0}^{\infty} u_n Y_n$ in $H^{1/2}(\Gamma_0)$, where

$$Z^n_{0,P} = \frac{(a_j + i\mu_n)(\tilde{a}_j + i\mu_n)}{(a_j - i\mu_n)(\tilde{a}_j - i\mu_n)}.$$

That is, u satisfies the CRBC (5.4) and (5.5) on Γ_0 if and only if u satisfies

$$\frac{\partial u}{\partial \nu} = T_{tc}(u) \text{ on } \Gamma_0. \tag{5.9}$$

Thus, approximate radiating solutions satisfying the CRBC on Γ_0 solve the weak problem

$$\mathcal{A}_{tc}(u, \phi) = (-f, \phi)_\Omega \text{ for } \phi \in H^1(\Omega), \tag{5.10}$$

where

$$\mathcal{A}_{tc}(u, \phi) = (\nabla u, \nabla\phi)_\Omega - k^2(u, \phi)_\Omega - \langle T_{tc}(u), \phi\rangle_{\Gamma_0}.$$

Since $\lim_{n\to\infty} Z_{0,P}^n = 1$ for given parameters a_j and $\tilde{a}_j$, the approximate DtN map T_{tc} does not converge to the exact DtN map T as operators from $H^{1/2}(\Gamma_0)$ to $H^{-1/2}(\Gamma_0)$. However, it is shown in [13] that T_{tc} converges to T for sufficiently smooth $\phi \in H^{1/2+s}(\Gamma_0)$ with $s > 0$, i.e., for any $n_p > 0$, there exists $M_0 = M_0(n_p) > N$ such that for any $M \geq M_0$ and $n_e > 0$ it holds that

$$\|(T - T_{tc})\phi\|^2_{H^{-1/2}(\Gamma_0)} \leq C\mathcal{E}(n_p, n_e, M)\|\phi\|^2_{H^{1/2+s}(\Gamma_0)}, \tag{5.11}$$

where

$$\mathcal{E}(n_p, n_e, M) \equiv (e^{-Cn_p/\ln(k/\mu_{min})} + e^{-Cn_e/\ln(\tilde{\mu}_M/\tilde{\mu}_{min})} + (1 + \lambda_M^2)^{-s})^{1/2}.$$

We note that $\mathcal{E}$ can be arbitrarily small by taking sufficiently large n_p, M and n_e due to (2.1) with k, μ_{min} and $\tilde{\mu}_{min}$ fixed. This convergence estimate plays an essential role for not only well-posedness of (5.10) but also the convergence of approximate solutions. In fact, the convergence result of (5.11) enables us to replace the DtN map T in (3.8), (4.1) and (4.4) by T_{tc} to find approximate solutions. The convergence analysis will be presented in the next subsection.

For computational purposes, CRBCs can be written in terms of auxiliary functions $\Phi = (\phi_0, \ldots, \phi_{P+1})^t \in (H^1(\Gamma_0))^{P+2}$ with $u = \phi_0$ on Γ_0 satisfying the system of differential equations

$$\begin{aligned} -\frac{\partial u}{\partial \nu}\boldsymbol{e}_0 &= -L\nabla_y^2\Phi + (-k^2L + M)\Phi \text{ on } \Gamma_0 \\ \frac{\partial \Phi}{\partial \nu} &= 0 \text{ on } \partial\Gamma_0, \end{aligned} \tag{5.12}$$

where $\boldsymbol{e}_j$ is the standard basis vector in $\mathbb{C}^{P+2}$ whose nonzero entry is one at the j-th component, L and M are $(P+2)\times(P+2)$ symmetric tridiagonal matrices whose nonzero entries are

$$\begin{aligned} L_{j,j-1} &= \frac{1}{a_{j-1} + \tilde{a}_{j-1}}, \quad L_{j,j} = \frac{1}{a_{j-1} + \tilde{a}_{j-1}} + \frac{1}{a_j + \tilde{a}_j}, \quad L_{j,j+1} = \frac{1}{a_j + \tilde{a}_j} \\ M_{j,j-1} &= \frac{-a_j^2}{a_{j-1} + \tilde{a}_{j-1}}, \quad M_{j,j} = \frac{a_{j-1}\tilde{a}_{j-1}}{a_{j-1} + \tilde{a}_{j-1}} + \frac{a_j\tilde{a}_j}{a_j + \tilde{a}_j}, \quad M_{j,j+1} = \frac{-\tilde{a}_j^2}{a_j + \tilde{a}_j} \end{aligned}$$

for $j = 0, \ldots, P+1$. Here we use the convention that the terms with indices out of the limits are ignored, for instance,

$$L_{0,0} = \frac{1}{a_0 + \tilde{a}_0} \quad \text{and} \quad L_{P+1,P+1} = \frac{1}{a_P + \tilde{a}_P}.$$

A derivation of (5.12) can be found in [13, 14].

Thus approximate radiating solutions to the problem (1.1) satisfying the CRBC on Γ_0 solve

$$\begin{aligned} &\Delta u + k^2 u = f \text{ in } \Omega, \\ &\quad \frac{\partial u}{\partial \nu}\boldsymbol{e}_0 = L\nabla_y^2\Phi + (k^2L - M)\Phi \text{ on } \Gamma_0 \quad \text{and} \quad \frac{\partial \Phi}{\partial \nu} = 0 \text{ on } \partial\Gamma_0. \end{aligned}$$

Denoting $\boldsymbol{V} = \{(u, \Phi) \in H^1(\Omega) \times (H^1(\Gamma_0))^{P+2} \; : \; u = \phi_0 \text{ on } \Gamma_0\}$, the variational reformulation can be written as finding $(u, \Phi) \in \boldsymbol{V}$ satisfying

$$\mathcal{A}_{pc}((u, \Phi), (\xi, \Psi)) = (-f, \xi)_\Omega \text{ for } (\xi, \Psi) \in \boldsymbol{V}, \tag{5.13}$$

where

$$\begin{aligned}\mathcal{A}_{pc}((u, \Phi), (\xi, \Psi)) = {} & (\nabla u, \nabla \xi)_\Omega - k^2 (u, \xi)_\Omega \\ & + \langle L \nabla_y \Phi, \nabla_y \Psi \rangle_{\Gamma_0} + \langle (-k^2 L + M)\Phi, \Psi \rangle_{\Gamma_0}.\end{aligned}$$

This formulation is well-suited for finding finite element approximations. By the equivalence between different representations of CRBCs, we can use (5.13) based on (5.12) for numerical computations but rely on another formulation (5.10) based on (5.9) for a convergence analysis (see [13]).

5.2. Algorithm for finding approximate solutions

Let $\mathrm{g}_0 = 0$ on Γ_0. For $j = 1, 2, \ldots, L-1$, we solve the problem

$$\begin{aligned}&\Delta \mathrm{w}_j + k^2 \mathrm{w}_j = f_j \text{ in } \Omega_j, \\ &\qquad \frac{\partial \mathrm{w}_j}{\partial \nu} = T_{tc}(\mathrm{w}_j) + \mathrm{g}_{j-1} \text{ on } \Gamma_{j-1} \text{ and } \frac{\partial \mathrm{w}_j}{\partial \nu} = T_{tc}(\mathrm{w}_j) \text{ on } \Gamma_j,\end{aligned} \tag{5.14}$$

where $\mathrm{g}_{j-1} = 2\partial \mathrm{w}_{j-1}/\partial \nu_{j,j-1}$ is the incoming data. The variational problem corresponding to the problem (5.14) is to find $\mathrm{w}_j \in H^1(\Omega_j)$ satisfying

$$\mathcal{A}_j(\mathrm{w}_j, \xi) = (-f_j, \xi)_{\Omega_j} + \langle \mathrm{g}_{j-1}, \xi \rangle_{\Gamma_{j-1}} \text{ for all } \xi \in H^1(\Omega_j), \tag{5.15}$$

where $\mathcal{A}_j(\cdot, \cdot)$ is a sesquilinear form defined in $H^1(\Omega_j) \times H^1(\Omega_j)$ by

$$\mathcal{A}_j(\phi, v) = (\nabla \phi, \nabla v)_{\Omega_j} - k^2 (\phi, v)_{\Omega_j} - \langle T_{tc}(\phi), \xi \rangle_{\Gamma_{j-1} \cup \Gamma_j} \tag{5.16}$$

for ϕ and $v \in H^1(\Omega_j)$. In [13], it is proved that the problem (5.15) is well-posed if n_p and n_e are sufficiently large. Also, the following is the result of Theorem 3.9 in [13] with Neumann incoming data.

Lemma 5.1. *Let $\tilde{w}_j \in H^{1+s}(\Omega_j)$, $0 < s \le 1$ and $\mathrm{w}_j \in H^1(\Omega_j)$ be the solutions to the problems* (3.8) *and* (5.14)*, respectively. Then for any $n_p > 0$, there exists $M_0 > N$ such that for any $M \ge M_0$ and $n_e > 0$ the error $\tilde{w}_j - \mathrm{w}_j$ satisfies*

$$\|\tilde{w}_j - \mathrm{w}_j\|_{H^1(\Omega_j)} \le C \left[\mathcal{E}(n_p, n_e, M) \|\tilde{w}_j\|_{H^{1+s}(\Omega_j)} + \|\tilde{g}_{j-1} - \mathrm{g}_{j-1}\|_{H^{-1/2}(\Gamma_{j-1})} \right]$$

for $j = 1, 2, \ldots, L$.

Using Lemma 5.1 inductively and a trace inequality yield the next lemma

Lemma 5.2. *Let* $\tilde{w}_j \in H^{1+s}(\Omega_j)$*,* $0 < s \le 1$ *and* $\mathrm{w}_j \in H^1(\Omega_j)$ *be the solutions to the problems* (3.8) *and* (5.14)*, respectively. Then for any* $n_p > 0$*, there exists* $M_0 > N$ *such that for any* $M \ge M_0$ *and* $n_e > 0$ *the error* $\tilde{w}_j - \mathrm{w}_j$ *satisfies*

$$\|\tilde{w}_j - \mathrm{w}_j\|_{H^1(\Omega_j)} \le C_j \mathcal{E}(n_p, n_e, M) \| \sum_{\ell=1}^{j} f_\ell \|_{L^2(\Omega)} \tag{5.17}$$

for $j = 1, 2, \ldots, L$*. Here* C_j *is a generic positive constant that may depend on* j *and a trace constant. Furthermore, by a trace inequality we have*

$$\|\tilde{g}_j - \mathrm{g}_j\|_{H^{-1/2}(\Gamma_j)} \le C_j \mathcal{E}(n_p, n_e, M) \| \sum_{\ell=1}^{j} f_\ell \|_{L^2(\Omega)}. \tag{5.18}$$

Proof. The proof proceeds by mathematical induction on j. For $j = 1$, since $\tilde{g}_0 = \mathrm{g}_0 = 0$ on Γ_0, we have

$$\|\tilde{w}_1 - \mathrm{w}_1\|_{H^1(\Omega_1)} \le C\mathcal{E} \|\tilde{w}_1\|_{H^{1+s}(\Omega_1)}$$

by Lemma 5.1 and, in turn, a trace inequality and the regularity of $\tilde{w}_1$ mentioned in Remark 3.4 show that

$$\|\tilde{g}_1 - \mathrm{g}_1\|_{H^{-1/2}(\Gamma_1)} \le C_1 \mathcal{E} \|f_1\|_{L^2(\Omega_1)}.$$

Assume that the estimates (5.17) and (5.18) hold for $j - 1 < L - 1$. Now, Lemma 5.1, Remark 3.4 and the inductive assumption prove that

$$\begin{aligned} \|\tilde{w}_j - \mathrm{w}_j\|_{H^1(\Omega_j)} &\le C \left[\mathcal{E} \|\tilde{w}_j\|_{H^{1+s}(\Omega_j)} + \|\tilde{g}_{j-1} - \mathrm{g}_{j-1}\|_{H^{-1/2}(\Gamma_{j-1})} \right] \\ &\le C \left[\mathcal{E} \| \sum_{\ell=1}^{j} f_\ell \|_{L^2(\Omega)} + C_{j-1} \mathcal{E} \| \sum_{\ell=1}^{j-1} f_\ell \|_{L^2(\Omega)} \right] \le C_j \mathcal{E} \| \sum_{\ell=1}^{j} f_\ell \|_{L^2(\Omega)} \end{aligned}$$

for some $C_j > 0$, which verifies the first estimate (5.17). Combining (5.17) and a trace inequality lead to (5.18), which completes the proof.

In backward sweeping to find the full wave expansion of approximate solutions, we consider the problem

$$\begin{aligned} \Delta \mathrm{z}_j + k^2 \mathrm{z}_j &= f_j \text{ in } \Omega_j, \\ \frac{\partial \mathrm{z}_j}{\partial \nu} &= T_{tc}(\mathrm{z}_j) + \mathrm{g}_{j-1} \text{ on } \Gamma_{j-1} \quad \text{and } \mathrm{z}_j = \mathrm{z}_{j+1} \text{ on } \Gamma_j \end{aligned} \tag{5.19}$$

for $j = 1, 2, \ldots, L - 1$ and

$$\begin{aligned} \Delta \mathrm{z}_L + k^2 \mathrm{z}_L &= f_L \text{ in } \Omega_L, \\ \frac{\partial \mathrm{z}_L}{\partial \nu} &= T_{tc}(\mathrm{z}_L) + \mathrm{g}_{L-1} \text{ on } \Gamma_{L-1}. \end{aligned} \tag{5.20}$$

It can be shown that the problem (5.19) is well-posed by the same idea as that used for the problem (5.15) (see [13]) with a standard solution estimation involving Dirichlet data on Γ_j, which is presented in the following lemma

Lemma 5.3. *Let* $z_j \in H^{1+s}(\Omega_j)$, $0 < s \le 1$ *and* $\mathrm{z}_j \in H^1(\Omega_j)$ *be the solutions to the problems* (4.4) *and* (5.19), *respectively. Then for any* $n_p > 0$, *there exists* $M_0 > N$ *such that for any* $M \ge M_0$ *and* $n_e > 0$, *the error* $z_j - \mathrm{z}_j$ *satisfies*

$$\|z_j - \mathrm{z}_j\|_{H^1(\Omega_j)} \le C\big[\mathcal{E}(n_p, n_e, M)\|z_j\|_{H^{1+s}(\Omega_j)} + \|g_{j-1} - \mathrm{g}_{j-1}\|_{H^{-1/2}(\Gamma_{j-1})} + \|z_{j+1} - \mathrm{z}_{j+1}\|_{H^{1/2}(\Gamma_j)}\big]$$

for $j = 1, 2, \ldots, L-1$.

Finally, we provide the convergence result of approximate solutions obtained by the sweeping algorithms. As mathematical induction with decreasing j can prove it in the same fashion as for Lemma 5.2, the proof is omitted here.

Theorem 5.4. *Let* $z_j \in H^{1+s}(\Omega_j)$, $0 < s \le 1$ *and* $\mathrm{z}_j \in H^1(\Omega_j)$ *be the solutions to the problems* (4.4) *and* (5.19), *respectively. Then for any* $n_p > 0$, *there exists* $M_0 > N$ *such that for any* $M \ge M_0$ *and* $n_e > 0$, *the error satisfies*

$$\|z_j - \mathrm{z}_j\|_{H^1(\Omega_j)} \le C_j \mathcal{E}(n_p, n_e, M)\|f\|_{L^2(\Omega)} \tag{5.21}$$

for $j = 1, 2, \ldots, L$. *Here* C_j *is a generic positive constant that may depend on* j *and a trace constant.*

We summarize the algorithm to find approximate solutions as follows:

Algorithm 3: to approximate solutions of the problem (1.1)

Step I: *Right sweeping to find the approximate incoming data* $\mathrm{g}_j = 2\partial \mathrm{w}_j/\partial \nu_{j+1,j}$ *for* $j = 0, 1, \ldots, L-1$*:*

- *(1)* *Set* $\mathrm{g}_0 = 0$.
- *(2)* *Do for* $j = 1, 2, \ldots, L-1$,
  - *i.* *Solve* (5.14) *for* w_j.
  - *ii.* *Compute* $\mathrm{g}_j = 2\dfrac{\partial \mathrm{w}_j}{\partial \nu_{j+1,j}} = -2\dfrac{\partial \mathrm{w}_j}{\partial x}$ *on* Γ_j.

  End do

Step II: *Left sweeping to find the approximate wave expansion* z_j *in* Ω_j *for* $j = L, \ldots, 2, 1$*:*

- *(1)* *Find* z_L *by solving the problem* (5.20) *in* Ω_L.
- *(2)* *Do for* $j = L-1, \ldots, 1$,
  - *i.* *Compute the Dirichlet data of* z_{j+1} *on* Γ_j.
  - *ii.* *Find* z_j *by solving the problem* (5.19) *in* Ω_j.

  End do

Remark 5.5. *When the domain* Ω *is a straight waveguide without a cavity, we can develop a Schwarz algorithm that can be easily parallelizable, i.e., we use a*

Jacobi-type nonoverlapping Schwarz method,

$$\begin{aligned}\Delta u_j^{m+1} + k^2 u_j^{m+1} &= f_j \ \textit{in } \Omega_j,\\ \frac{\partial u_j^{m+1}}{\partial \nu_{j,j-1}} &= T(u_j^{m+1}) + g_j^{W,m} \ \textit{on } \Gamma_{j-1},\\ \frac{\partial u_j^{m+1}}{\partial \nu_{j,j+1}} &= T(u_j^{m+1}) + g_j^{E,m} \ \textit{on } \Gamma_j,\end{aligned}$$

where m stands for the iteration number. Here $g_j^{W,m}$ and $g_j^{E,m}$ are Neumann data of wave fields coming into the domain Ω_j through Γ_{j-1} and Γ_j, respectively and they are determined by

$$g_j^{W,m} = \frac{\partial u_{j-1}^m}{\partial \nu_{j,j-1}} - T(u_{j-1}^m) \quad \textit{and} \quad g_j^{E,m} = \frac{\partial u_{j+1}^m}{\partial \nu_{j,j+1}} - T(u_{j+1}^m).$$

In fact, $g_j^{W,m}$ ($g_j^{E,m}$) is the Neumann data of the right-going (left-going) component of u_{j-1}^m (u_{j+1}^m) multiplied by -2 and they are the incoming sources for the subdomain problem as seen in (3.4) *with $\nu = \nu_{j,j\pm 1}$. Now, this Schwarz iteration formula can be approximated by replacing the DtN map T by CRBCs T_{tc} as done for the double sweeping Algorithm 3. It is worth noting that [5] proposed a similar Jacobi-type Schwarz method transferring data associated with auxiliary functions instead of Neumann data on physical boundaries Γ_j. There, it is addressed that a stability issue might arise in finding incoming data from a system of equations involving auxiliary functions on interfaces as seen in Fig. 7 of [4], however this new approach exploiting Neumann data on physical boundaries can get rid of this stability problem.*

6. Implementation of the algorithm

As addressed in Subsection 5.1, when we seek for solutions w_j to the problem (5.14) and z_j to (5.19) and (5.20), we apply the finite element method to the weak problems based on (5.12). For the problem (5.14) in the right sweeping process of Step I, the test space $\boldsymbol{V}$ is defined by

$$\begin{aligned}\boldsymbol{V} = \{(u, \Phi^W, \Phi^E) \in H^1(\Omega_j) \times (H^1(\Gamma_{j-1}))^{P+2} \times (H^1(\Gamma_j))^{P+2} \ :\\ u = \phi_0^W \text{ on } \Gamma_{j-1} \text{ and } u = \phi_0^E \text{ on } \Gamma_j\},\end{aligned}$$

where $\Phi^W = (\phi_0^W, \ldots, \phi_{P+1}^W)^t$ and $\Phi^E = (\phi_0^E, \ldots, \phi_{P+1}^E)^t$, and the sesquilinear form is given by

$$\begin{aligned}\mathcal{A}_{pc}((u, \Phi^W, \Phi^E), (\xi, \Psi^W, \Phi^E)) &= (\nabla u, \nabla \xi)_{\Omega_j} - k^2 (u, \xi)_{\Omega_j}\\ &+ \langle L \nabla_y \Phi^W, \nabla_y \Psi^W \rangle_{\Gamma_{j-1}} + \langle (-k^2 L + M)\Phi^W, \Psi^W \rangle_{\Gamma_{j-1}}\\ &+ \langle L \nabla_y \Phi^E, \nabla_y \Psi^E \rangle_{\Gamma_j} + \langle (-k^2 L + M)\Phi^E, \Psi^E \rangle_{\Gamma_j}.\end{aligned}$$

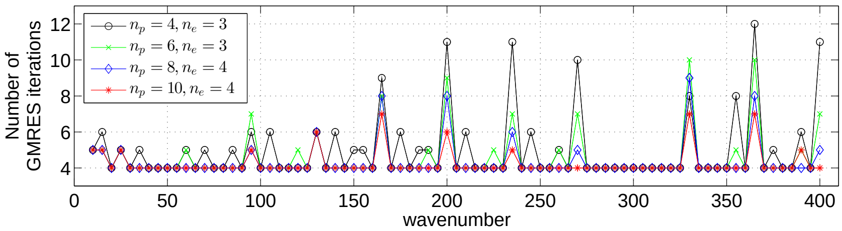

Figure 2: Number of GMRES iterations vs. wavenumber.

Then weak solutions to the problem (5.14) are obtained by solving the problem

$$\mathcal{A}_{pc}((\mathrm{w}_j, \Phi^W, \Phi^E), (\xi, \Psi^W, \Psi^E)) = (-f_j, \xi)_{\Omega_j} + \langle \mathrm{g}_{j-1}, \xi\rangle_{\Gamma_{j-1}} \text{ for } (\xi, \Psi^W, \Psi^E) \in \boldsymbol{V} \tag{6.1}$$

for $j = 1, 2, \ldots, L-1$.

Now, we discuss about how to compute the right-hand-side vectors of (6.1) involving data g_{j-1} in finite element implementations. We recall that the date g_{j-1} are given by

$$\mathrm{g}_{j-1} = 2\frac{\partial \mathrm{w}_{j-1}}{\partial \nu_{j,j-1}} = -2\frac{\partial \mathrm{w}_{j-1}}{\partial \nu_{j-1,j}} \text{ on } \Gamma_{j-1}.$$

Let $\vartheta_1, \ldots, \vartheta_J$ be nodal basis functions on Γ_{j-1} and denote the $J \times J$ mass and stiffness matrices on Γ_{j-1} by $\mathcal{M}$ and $\mathcal{S}$, respectively. Here all we need is L^2-inner products of the finite element approximation of g_{j-1} with finite element basis functions in Γ_{j-1}, i.e, if we denote the coefficient vector of the finite element approximation of g_{j-1} by $\mathfrak{g}$, then we need to find $\mathcal{M}\mathfrak{g}$. Assume that the finite element solution for $(\mathrm{w}_{j-1}, \Phi^W, \Phi^E)$ satisfying (6.1) in the subdomain Ω_{j-1} is at hand and hence we have coefficient vectors for the finite element approximations of ϕ_0^E and ϕ_1^E on Γ_{j-1}, denoted by $\mathfrak{u}_0$ and $\mathfrak{u}_1$ with respect to $\vartheta_1, \ldots, \vartheta_J$, respectively.

Now, the computation of $\mathcal{M}\mathfrak{g}$ can be performed as follows. The zero-th equation of the system of equations in (5.12) with Γ_0 replaced by Γ_{j-1} reads

$$-\frac{\partial \mathrm{w}_{j-1}}{\partial \nu_{j-1,j}} = -L_{0,0}\nabla_y^2\phi_0^E - L_{0,1}\nabla_y^2\phi_1^E + (-k^2L_{0,0}+M_{0,0})\phi_0^E + (-k^2L_{0,1}+M_{0,1})\phi_1^E,$$

which implies that for $\xi \in H^1(\Gamma_{j-1})$

$$\begin{aligned}-\langle\frac{\partial \mathrm{w}_{j-1}}{\partial \nu_{j-1,j}}, \xi\rangle_{\Gamma_{j-1}} &= L_{0,0}\langle\nabla_y\phi_0^E, \nabla_y\xi\rangle_{\Gamma_{j-1}} + L_{0,1}\langle\nabla_y\phi_1^E, \nabla_y\xi\rangle_{\Gamma_{j-1}} \\ &+ (-k^2L_{0,0} + M_{0,0})\langle\phi_0^E, \xi\rangle_{\Gamma_{j-1}} + (-k^2L_{0,1} + M_{0,1})\langle\phi_1^E, \xi\rangle_{\Gamma_{j-1}}.\end{aligned}$$

Since the corresponding finite element approximations $\mathfrak{g}$, $\mathfrak{u}_0$ and $\mathfrak{u}_1$ satisfy

$$\frac{1}{2}\mathcal{M}\mathfrak{g} = (L_{0,0}\mathcal{S} + (-k^2L_{0,0}+M_{0,0})\mathcal{M})\mathfrak{u}_0 + (L_{0,1}\mathcal{S} + (-k^2L_{0,1}+M_{0,1})\mathcal{M})\mathfrak{u}_1, \tag{6.2}$$

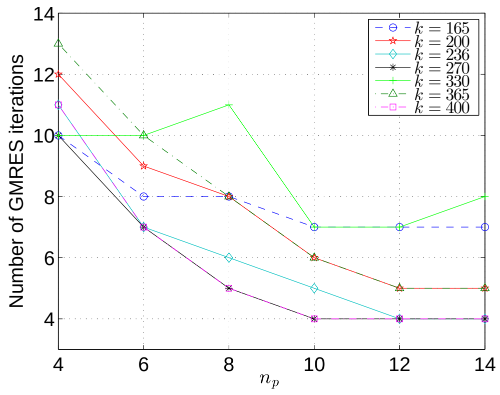

Figure 3: Number of GMRES iterations vs. CRBC orders with (n_p, n_e) =(4,2),(6,3),(8,3),(10,4),(12,4) and (14,5).

we can construct the right-hand-side vector of the finite element problem for (6.1). Here it is worth pointing out that we might use approximate Neumann data by using the first or second order backward difference formulas (BDF or BDF2) but they introduce another approximation error to solutions, which results in slow convergence of GMRES iterations as will be seen in numerical experiments.

In the left sweeping process of Step II, we solve the problems (5.19) and (5.20). In this case, the solution space $\boldsymbol{V}$ and test space $\widetilde{\boldsymbol{V}}$ are defined by

$$\boldsymbol{V} = \{(u, \Phi^W) \in H^1(\Omega_j) \times (H^1(\Gamma_{j-1}))^{P+2} \ : \ u = \phi_0^W \text{ on } \Gamma_{j-1}\},$$
$$\widetilde{\boldsymbol{V}} = \begin{cases} \{(u, \Phi^W) \in \boldsymbol{V} \ : \ u = 0 \text{ on } \Gamma_j\} & \text{if } 1 \le j < L, \\ \boldsymbol{V} & \text{if } j = L. \end{cases}$$

We seek for weak solutions $(\mathrm{z}_j, \Phi^W) \in \boldsymbol{V}$ to (5.19) such that $\mathrm{z}_j = \mathrm{z}_{j+1}$ on Γ_j (if $j \neq L$) and

$$\mathcal{A}_{pc}((\mathrm{z}_j, \Phi^W), (\xi, \Psi^W)) = (-f_j, \xi)_{\Omega_j} + \langle \mathrm{g}_{j-1}, \xi \rangle_{\Gamma_{j-1}} \text{ for } (\xi, \Psi^W) \in \widetilde{\boldsymbol{V}},$$

where

$$\mathcal{A}_{pc}((u, \Phi^W), (\xi, \Psi^W)) = (\nabla u, \nabla \xi)_{\Omega_j} - k^2 (u, \xi)_{\Omega_j} + \langle L \nabla_y \Phi^W, \nabla_y \Psi^W \rangle_{\Gamma_{j-1}} + \langle (-k^2 L + M) \Phi^W, \Psi^W \rangle_{\Gamma_{j-1}}.$$

7. Numerical experiments

We first consider the model problem

$$\begin{aligned} \Delta u + k^2 u = f \text{ in } \Omega, \\ \frac{\partial u}{\partial \nu} = 0 \text{ on } \Omega \setminus \bar{\Gamma}_0 \ \text{ and } \ \frac{\partial u}{\partial \nu} = T(u) \text{ on } \Gamma_0, \end{aligned} \tag{7.1}$$

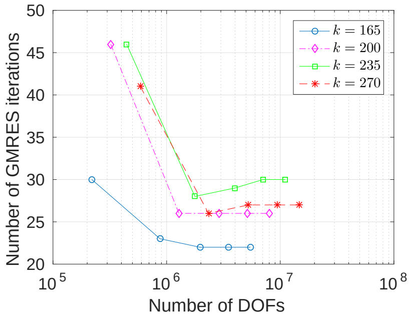

(a) vs. mesh density with $(n_p, n_e) = (1, 0)$

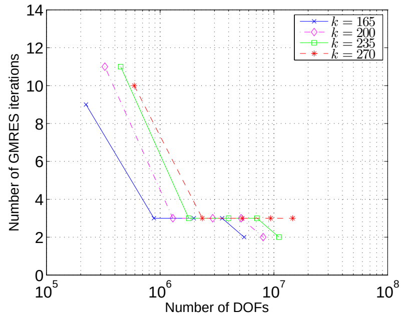

(b) vs. mesh density with $(n_p, n_e) = (4, 3)$

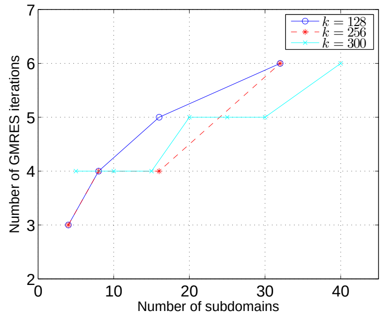

(c) vs. number of subdomains

Figure 4: Number of GMRES iterations: (a), (b) vs. mesh density ($q = 2, 4, 6, 8$, and 10) with CRBC order $(n_p, n_e) = (1, 0)$ and $(n_p, n_e) = (4, 3)$, respectively (c) vs. number of subdomains for $k = 128, 256, 300$ with the CRBC of order $(n_p, n_e) = (4, 3)$ and $q = 2$.

where $\Omega = (0, 1) \times (0, 1) \subset \mathbb{R}^2$ and f is a point source at two points $(0.0312, 0.6)$ and $(0.3245, 0.4)$. The optimized double sweep Schwarz method is tested for solving the above problem for $k = 10, 15, \ldots, 400$. The domain Ω is decomposed into 10 nonoverlapping equal-sized layered subdomains along the x-axis. We use the finite element library `deal.II` [23] to find finite element approximations with mesh size h determined by the rule of thumb that a certain number of grid points per wave length are required for acceptable accuracy, for instance, $h = 1/(2k)$ leads to approximately 12 grid points assigned for a wavelength along the x-axis. It is worth noting that the size of local problems involved in the right-sweeping process of the algorithm based on CRBC is only half of that in STDDM proposed in [9].

By using CRBCs of order $(n_p, n_e) = (4, 3), (6, 3), (8, 4)$ and $(10, 4)$ (both on the interfaces Γ_j for $j = 1, 2, \ldots, L-1$ and on the boundary Γ_0 of Ω), we obtain the number of preconditioned GMRES iterations presented in Figure 2 illustrating that they reach the stopping criterion only at 4 or 5 iterations for most wavenumbers except a few peaks. In these tests, iterations stop when relative residuals are less than 10^{-6}. Furthermore, it can be seen that the peaks

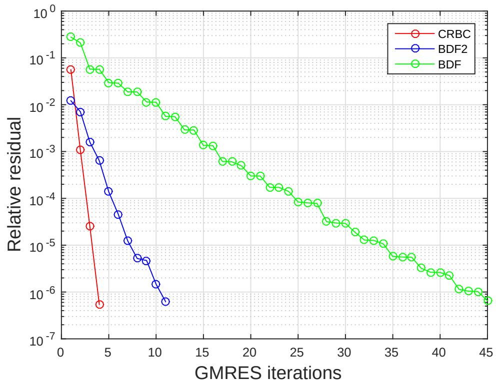

Figure 5: Relative residual vs. GMRES iterations with Neumann data obtained by (6.2), BDF and BDF2.

can be removed by taking higher order CRBCs, and GMRES iterations with respect to CRBC orders for those wavenumbers pertaining to the peaks are presented in Figure 3.

For a fixed CRBC, we can also reduce the number of preconditioned GMRES iterations by choosing the larger mesh density, that is by introducing a parameter q for mesh density defined by $h = 1/(kq)$ for $q = 2, 4, 6, 8$ and 10. The results with respect to the mesh density (and hence degrees of freedom) are reported in Figure 4 (a) and (b). In Figure 4(a) for a low-order CRBC of order $(n_p, n_e) = (1, 0)$, the finer mesh does not guarantee the faster convergence since the reflection errors dominate the mesh errors in this case however, as seen in Figure 4(b) for a high-order CRBC of order $(n_p, n_e) = (4, 3)$ generating the reflection errors ignorable compared with the mesh errors, less iterations are needed in the finer meshes.

Figure 4(c) shows the number of preconditioned GMRES iterations with respect to the number of subregions of decomposition of Ω. The domain Ω is split into 4, 8, 16, and 32 subdomains for $k = 128$ and 256 and into 5, 10, 15, 20, 25 and 30 for $k = 300$. It can be seen that the number iterations increase mildly with the number of subregions

In the next example, we examine the performance of the double sweeping algorithm in terms of incoming Neumann data obtained by three difference methods such as the formula (6.2) (based on CRBC), BDF and BDF2. To do this, we consider the model problem (7.1) with $k = 50$ but we assume that $f = 0$ and an incident wave field u^{in} given by

$$u^{in}(x, y) = \sum_{n=0}^{10} e^{i\mu_n x} Y_n(y)$$

is coming into the domain Ω through the boundary Γ_0. We take the mesh size $h = 1/(2k)$ and CRBC of order $(n_p, n_e) = (4, 1)$. Figure 6 illustrates the graphs

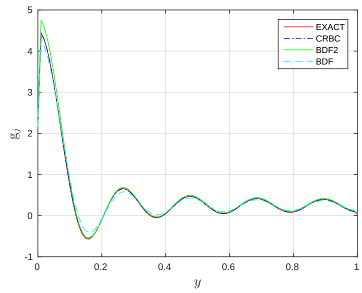

(a) g_1 on Γ_1

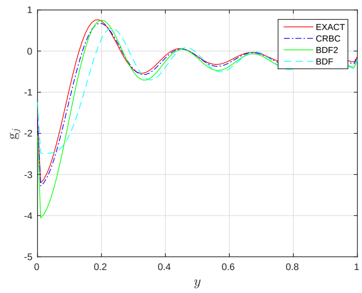

(b) g_3 on Γ_3

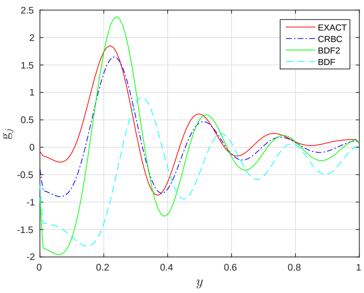

(c) g_7 on Γ_7

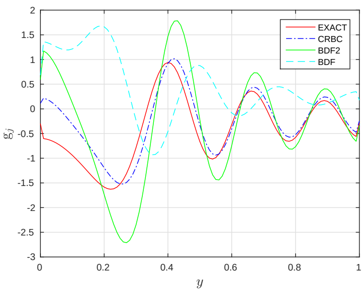

(d) g_9 on Γ_9

Figure 6: Computation of g_1 by three different methods: (6.2) based on CRBC, BDF and BDF2.

of g_j on Γ_j computed by three different methods, (6.2), BDF and BDF2. It shows that all computations of g_1 on Γ_1 agree well with the exact g_1, however as the forward sweeping algorithm proceeds their errors are getting larger. It is observed that the results of (6.2) appear to have a good agreement with the exact Neumann data even on Γ_9 while the results of BDF and BDF2 on Γ_9 (in particular one for BDF) show significant difference from the exact g_9, which results in slow convergence of GMRES iterations. The relative residual with respect to GMRES iterations for each case can be found in Figure 5, in which we can see that the GMRES iterations obtained by (6.2) converge much faster than others obtained by BDF or BDF2.

In the final example, we are concerned with implementation of the optimized double sweep Schwarz method in case that scatterers are placed in the middle of an infinite waveguide. Let $k = 500$ and Ω be the complement of the three square obstacles of width 0.1 on the symmetric axis $x = 0$ in the domain $(-0.5, 0, 5) \times (0, 1)$ as in Figure 7. The point sources are located at $(-0.3312, 0.6)$ and $(0.3245, 0.4)$ and the CRBCs of order $(n_p, n_e) = (4, 3)$ are imposed on the artificial boundaries on $x = \pm 0.5$. We decompose the computational domain Ω into $2L - 1$ subdomains in a way that three obstacles are included in a single subregion $\Omega_L = \Omega^L$, the subregions on the left side of Ω_L

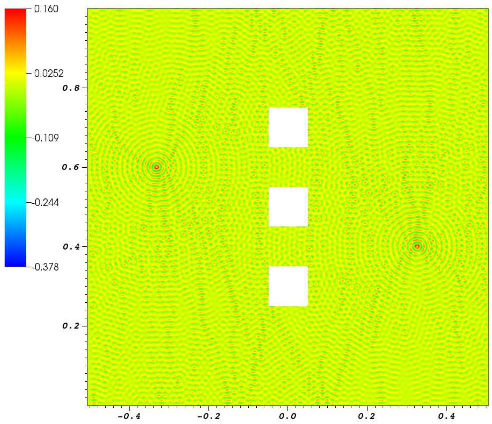

Figure 7: Snapshot of the real part of wave fields generated by point sources when three square obstacles are placed in the infinite waveguide $\mathbb{R} \times (0, 1)$.

are denoted by $\Omega_1, \Omega_2, \ldots, \Omega_{L-1}$ and those on the right of Ω^L are denoted by $\Omega^{L-1}, \Omega^{L-2}, \ldots, \Omega^1$. Now, application of Step I of *Algorithm 3* to both sides of Ω_L yields the collection of incoming data g_j from Ω_j and g^j from Ω^j, and then we solve the problem in $\Omega_L = \Omega^L$ with the incoming data g_{L-1} and g^{L-1} on the left and right boundaries of Ω_L, respectively. Finally, with the Dirichlet data of the solution obtained from the domain $\Omega_L = \Omega^L$ we follow the step II of *Algorithm 3* on both sides to have the approximate solution in the whole domain Ω. In this example, the domain Ω is decomposed into 9 subdomains among which 8 subdomains of width 0.1 are identical and the rest is the rectangular domain $(-0.1, 0.1) \times (0, 1)$ minus the three obstacles. Taking the CRBC of order $(4, 3)$ and the mesh density $q = 2$, the preconditioned GMRES iterations satisfy the relative residual less than the tolerance 10^{-6} at the third iterate and the snapshot of the real part of the solution is given in Figure 7.

8. Acknowledgments

This research of the first author was supported by Basic Science Research Program through the National Research Foundation of Korea (NRF) funded by the Ministry of Education, Science and Technology (2015R1D1A1A01057350)

[1] M. J. Gander, F. Magoulès, F. Nataf, Optimized Schwarz methods without overlap for the Helmholtz equation, SIAM J. Sci. Comput. 24 (1) (2002) 38–60 (electronic).

[2] M. J. Gander, Optimized Schwarz methods, SIAM J. Numer. Anal. 44 (2) (2006) 699–731.

[3] Y. Boubendir, X. Antoine, C. Geuzaine, A quasi-optimal non-overlapping domain decomposition algorithm for the Helmholtz equation, J. Comput. Phys. 231 (2) (2012) 262–280.

[4] M. J. Gander, L. Halpern, F. Magoulès, An optimized Schwarz method with two-sided Robin transmission conditions for the Helmholtz equation, Internat. J. Numer. Methods Fluids 55 (2) (2007) 163–175.

[5] S. Kim, H. Zhang, Optimized Schwarz method with complete radiation transmission conditions for the Helmholtz equation in waveguides, SIAM J. Numer. Anal. 53 (3) (2015) 1537–1558.

[6] Z. Chen, M. J. Gander, H. Zhang, On the relation between optimized Schwarz methods and source transfer, in: Domain Decomposition Methods in Science and Engineering XXII, Vol. 104 of Lect. Notes Comput. Sci. Eng., Springer, Berlin, 2016, pp. 217–225.

[7] M. J. Gander, F. Nataf, An incomplete LU preconditioner for problems in acoustics, J. Comput. Acoust. 13 (3) (2005) 455–476.

[8] B. Engquist, L. Ying, Sweeping preconditioner for the Helmholtz equation: moving perfectly matched layers, Multiscale Model. Simul. 9 (2) (2011) 686–710.

[9] Z. Chen, X. Xiang, A source transfer domain decomposition method for Helmholtz equations in unbounded domain, SIAM J. Numer. Anal. 51 (4) (2013) 2331–2356.

[10] C. C. Stolk, A rapidly converging domain decomposition method for the Helmholtz equation, J. Comput. Phys. 241 (0) (2013) 240 – 252.

[11] A. Vion, C. Geuzaine, Double sweep preconditioner for optimized Schwarz methods applied to the Helmholtz problem, J. Comput. Phys. 266 (2014) 171–190.

[12] F. Magoulès, P. Iványi, B. H. V. Topping, Non-overlapping Schwarz methods with optimized transmission conditions for the Helmholtz equation, Comput. Methods Appl. Mech. Engrg. 193 (45-47) (2004) 4797–4818.

[13] S. Kim, Analysis of complete radiation boundary conditions for the Helmholtz equation in perturbed waveguides, manuscript.

[14] S. Kim, T. Hagstrom, Complete radiation boundary conditions for the Helmholtz equation I: waveguides, manuscript.

[15] R. L. Higdon, Absorbing boundary conditions for difference approximations to the multidimensional wave equation, Math. Comp. 47 (176) (1986) 437–459.

[16] R. L. Higdon, Numerical absorbing boundary conditions for the wave equation, Math. Comp. 49 (179) (1987) 65–90.

[17] R. Courant, D. Hilbert, Methods of Mathematical Physics, Vol. 1, Wiley-Interscience, New York, 1953.

[18] C. I. Goldstein, A finite element method for solving Helmholtz type equations in waveguides and other unbounded domains, Math. Comp. 39 (160) (1982) 309–324.

[19] E. Bécache, A.-S. Bonnet-Ben Dhia, G. Legendre, Perfectly matched layers for the convected Helmholtz equation, SIAM J. Numer. Anal. 42 (1) (2004) 409–433.

[20] A. Bendali, P. Guillaume, Non-reflecting boundary conditions for waveguides, Math. Comp. 68 (225) (1999) 123–144.

[21] F. Nataf, F. Rogier, E. de Sturler, Optimal interface conditions for domain decomposition methods, Tech. Rep. Internal report No. 301, CMAP, Ecole Polytechnique (1994).

[22] P. Petrushev, V. Popov, Rational Approximation of Real Functions, Vol. 28 of Encyclopedia of Mathematics, Cambridge University Press, Cambridge, 1987.

[23] W. Bangerth, R. Hartmann, G. Kanschat, deal.II—a general-purpose object-oriented finite element library, ACM Trans. Math. Software 33 (4) (2007) 24.